Stress Corrosion Cracking of Superplastically Formed 7475 Aluminum Alloy

T.C. TSAI, J.C. CHANG, and T.H. CHUANG

The effects of biaxial superplastic deformation and postforming heat treatment upon the stress corrosion cracking (SCC) of a fine-grained 7475Al alloy plate have been investigated. For all postforming tempered conditions, increasing the extent of superplastic deformation, which created more cavitations, would decrease the mechanical properties, the SCC resistance, and the corrosion resistance. The influence of cavitation on the decay of elongation of the superplastically formed workpieces is larger than that on the decay of its strength. Post-forming tempered by retrogression and reaging (RRA) treatment could effectively improve the SCC resistance of workpieces in postforming T6 temper while not sacrificing the strength. However, the benefit of improving the SCC resistance by means of the postforming RRA temper was decreased with increasing the extent of superplastic deformation, because the SCC susceptibility increased as the extent of superplastic deformation increased for each postforming tempered condition. The cavitation led to more anodic corrosion potential and pitting potential and to an increase in both corrosion current density and passive current density, which would increase the SCC susceptibility.

I. INTRODUCTION

THERMOMECHANICAL treatment has been employed to produce a fine grain size in high-strength 7475Al alloy,[1] which possessed superplasticity.[2] The substantial advantages for fabrication of aerospace components by superplastic forming in comparison with conventional fabrication methods are lower weight, lower production cost, less wastage, and more efficient design. However, an undesirable phenomenon for the superplastic forming of a fine-grained 7475Al alloy is the formation of cavitation,[3,4] which will reduce the subsequent mechanical properties.[5] Furthermore, it is well known that 7*xxx* series aluminum alloys are susceptible to stress corrosion cracking (SCC) failures observed in service, particularly when they are aged to the near-peak-strength T6 tempered condition.[6] Recent studies have also shown that in a T6 tempered 7475Al alloy, prior superplastic deformation has been found to suffer atmospheric SCC.[7] For the same reason, a possible degradation of SCC resistance, when the superplastically formed 7475Al alloy is used for structural aerospace components, could be particularly serious.

Burleigh[8] summarized that the main mechanism for SCC in 7*xxx* series aluminum is hydrogen-induced cracking. Generally, the increase of matrix precipitate size and the associated change from GP zones to semicoherent η' and incoherent η precipitates will result in a more homogeneous slip mode and the reduction of slip planarity.[9] The homogeneous slip mode can effectively reduce hydrogen transported to the grain boundaries for inducing cracking by means of mobile dislocations.[9,10] On the other hand, the larger grain boundary precipitates (GBPs) can act as trapping sites for atomic hydrogen to retard intergranular SCC.[11,12] By trapping atomic hydrogen, the bubbles of molecular hydrogen nucleate at GBPs, thus lowering the concentration of atomic hydrogen in the grain boundary and preventing hydrogen embrittlement, which is due to atomic hydrogen reducing grain boundary cohesion.[12,13] An *RRA*[14] heat treatment was claimed to give SCC resistance equivalent to that of T73 temper together with T6 strength level.[11,15,16] The RRA tempered condition can provide a larger size of GBPs to reduce SCC susceptibility[8,11] and a greater volume fraction of coherent matrix precipitates to retard the loss of strength[16] than can the T6 tempered condition.

Previous investigations have paid much attention to the effects of superplastic deformation on the subsequent service mechanical properties.[5,17,18] However, it is very rare to report on the SCC testing. The purpose of this investigation was to evaluate the influences of different amounts of superplastic deformation and various postforming heat treatments on SCC susceptibility of superplastically formed workpieces.

II. EXPERIMENTAL PROCEDURE

The commercial 2-mm-thick superplastic 7475Al alloy plate was used in this investigation. The chemical compositions are listed in Table I. A metallographic photograph of the as-received 7475Al alloy plate reveals a fine-grained microstructure, as shown in Figure 1. The mean intercept grain dimensions for this alloy are $12.5 \times 12.1 \times 9.2$ μm.

The superplastic 7475Al plate was cut to obtain some disk specimens with a diameter of 13 cm. The disk specimens were superplastically bulge formed into a cylindrical die by using high-purity argon. The pan-shaped workpieces were formed at 515 °C, under 40 psi argon pressure for 30 minutes, then cooled in air. These workpieces possessed 11 cm diameter and different forming heights of 1, 2, and 3 cm, respectively. Three kinds of the pan-shaped specimens were treated by post-forming heat-treatment procedures, which were T6, RRA, and T73 tempers, as described in

T.C. TSAI, Postdoctor, J.C. CHANG, Doctoral Candidate, and T.H. CHUANG, Professor, are with the Institute of Materials Science and Engineering, National Taiwan University, Taiwan, 106, Republic of China.

Manuscript submitted October 23, 1996.

Table I. Chemical Compositions (Weight Percent) of the 7475 Aluminum Alloy

Alloy	Zn	Mg	Cu	Cr	Fe	Si	Mn	Ti	Al
7475	5.80	2.24	1.53	0.19	0.08	0.02	0.01	0.02	bal

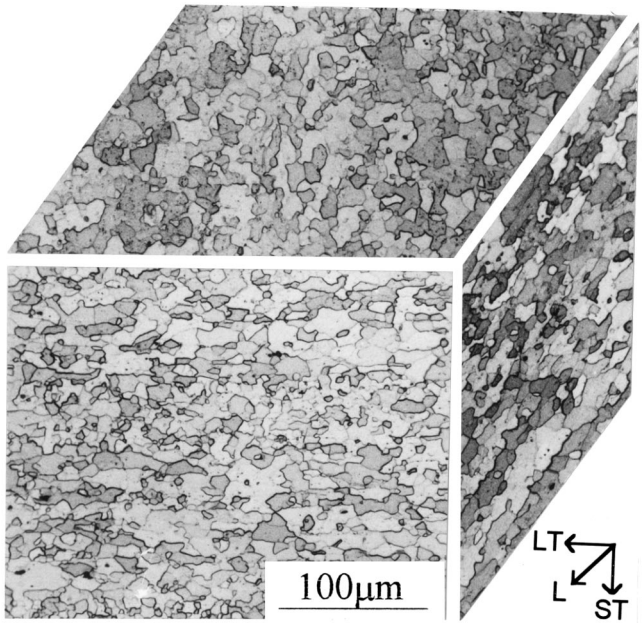

Fig. 1—Three-dimensional micrograph showing grain structure of the as-received 7475 alloy plate.

Table II. All tempered conditions for the different extents of superplastic deformation in this study are shown in Table III.

Rectangular tensile specimens with longitudinal direction, cut through the central section of the pan bottom, for each tempered condition were used to measure mechanical properties and aqueous SCC resistances. The tensile specimens were milled to 25-mm gage length, 6-mm width, and 1-mm thickness. Tensile tests were performed at a strain rate of 10^{-3} s^{-1} in air to obtain 0.2 pct offset yield strength, tensile strength, and elongation. The SCC tests were evaluated by using a slow strain rate test (SSRT).[19] The SSRT has the advantage that it will promote SCC in systems that in static tests either do not crack or take a particularly long time to show evidence of failure. The specimens of SSRT were tested at a strain rate of 4×10^{-6} s^{-1} in air and in near-neutral 3.5 pct NaCl aqueous solution (pH = 6.8), respectively. The SCC susceptibility for all tempered conditions could be evaluated by means of comparing their elongation losses, which were calculated by the elongations of testing in air, and those of testing in 3.5 pct NaCl solution.

The specimen, cut from the central section of the pan bottom, for each tempered condition was employed to measure the electrochemical properties by using a potentiodynamic polarization technique. Each specimen was polished with abrasive paper to 600 grit, then rinsed in acetone and washed in distilled water. The surface area of the working electrode was 25 mm^2. The potentiodynamic polarization tests were conducted in a cell containing aerated 3.5 pct NaCl solution (same as the aqueous SCC testing environment) at room temperature. This cell was equipped with a saturated calomel reference electrode and a platinum auxiliary electrode. Before polarization tests, the specimens were cathodically polarized at a constant potential of −1500 mV for 5 minutes to clean the electrode surface. Then, potentiodynamic scanning at a rate of 1 mV/s, from cathodic toward anodic direction, was applied to obtain the polarization curves.

Table II. Postforming Heat-Treatment Procedures of the Superplastically Formed Workpieces*

Temper	Condition	Aging Treatment
T6	near peakaged	24 h/120 °C
RRA	peakaged	T6 aged + 5 min/220 °C + T6 aged
T73	overaged	6 h/107 °C + 24 h/163 °C

*Solution treated at 515 °C for 1.5 h + water quenched.

Table III. Cavitation Volume Fraction of Superplastically Formed Workpieces with Various ETS*

	ETS = 20 Pct	ETS = 50 Pct	ETS = 100 Pct
Cavitation $\Delta V/V$ (Pct)	0.07 ± 0.02	0.14 ± 0.02	0.19 ± 0.03

*Data indicate mean ± 1 standard deviation.

The extent of cavitation for the pan-shaped workpiece was quantitatively evaluated by comparing the density loss with unformed material. At least five samples for each forming height workpiece, from the central to the corner section of the pan bottom, were cut to measure the densities. Using a suspended flotation technique, the specimen densities were measured by comparison with an equal density mixture of two organic liquids (diiodomethane and iodoethane).[5,20] The densities of mixtures were obtained by pycnometry.[21] All testing specimens were treated by T6 temper before measuring densities to avoid the influence of different heat-treatment procedures.[5,20]

A JEOL 100CXII transmission electron microscope operating at 100 kV was utilized to observe the microstructural change. Thin foils were prepared by twin-jet electropolishing in a 33 pct HNO_3 + 67 pct methanol solution cooled to −25 °C, using a potential of ~12 V. Fractography of the SCC and corrosion testing specimens was conducted with a PHILIPS* SEM515 scanning electron microscope operating at 20 kV.

*PHILIPS is a trademark of Philips Electronic Instruments Corp., Mahwah, NJ.

III. RESULTS

The typical pan-shaped workpieces with the different forming heights and their central cross-sectional profiles are shown in Figures 2(a) and (b), respectively. Figure 2(b) indicates that the forming thicknesses of the pan-shaped specimens are decreased with increasing the forming height, and their thickness distributions are not uniform. The amount of superplastic strain for each pan-shaped workpiece was evaluated as an equivalent tensile strain (ETS) by using the following relationship:[18]

$$\text{ETS pct} = (t_0/t_f - 1) \times 100$$

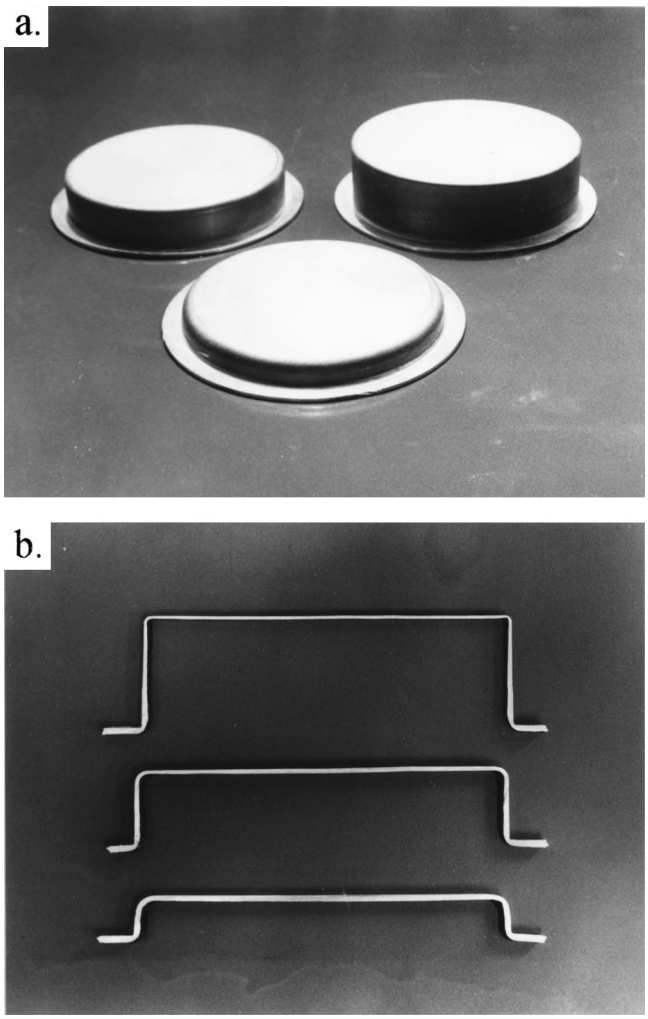

Fig. 2—(*a*) The pan-shaped specimens with the different forming heights. (*b*) The central cross-sectional profiles of the pan-shaped specimens.

where t_0 is the thickness of the plate before forming (2 mm), and t_f is the thickness of the plate after forming.

The average forming thickness of the workpiece bottom was used to calculate the ETS in this study. The approximate ETS for the different forming heights with 1, 2, and 3 cm are 20, 50, and 100 pct, respectively. Figure 3 shows the cavitation distributions around the central section of the pan bottom for the different forming height workpieces. It can be found that the cavitations almost nucleated at grain boundaries, and the larger and more evident cavitations increased with increasing the forming height, as indicated in Figure 3. The cavitation volume fractions for the various extents of superplastic deformation are shown in Table III. It demonstrates that the cavitation is increased with increasing the amount of ETS.

Before and after all postforming heat treatments, the mechanical properties of the pan-shaped specimens with different ETSs are shown in Table IV. The following points should be noted from Table IV:

(1) The yield strengths of the pan-shaped workpieces without any postforming temper were lower than 200 MPa. After postforming temper, the strengths of the pan-shaped samples could largely be increased to higher than 400 MPa. These results demonstrate that the superplastically formed workpieces can only be applied after the post-forming tempered treatment.

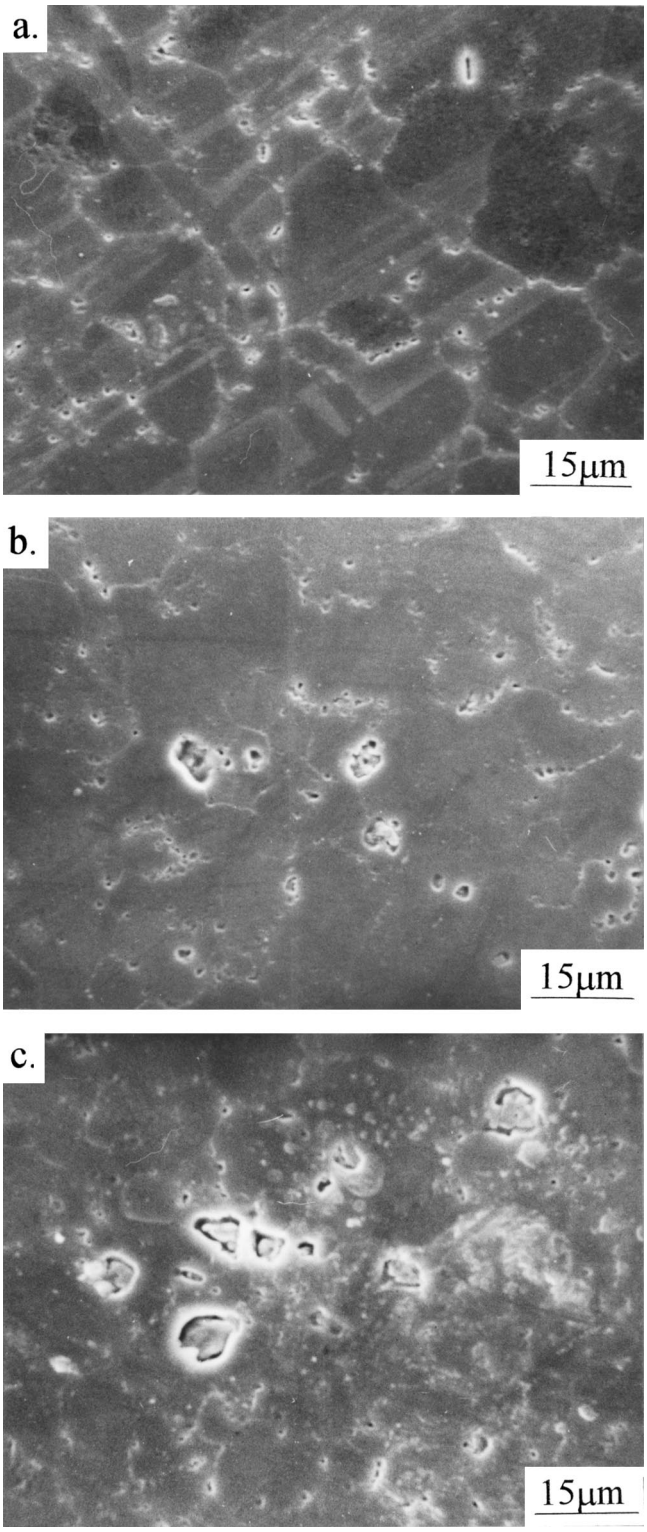

Fig. 3—The typical cavitation distributions around the central section of the bottom of the pan-shaped specimens for the different forming heights. (*a*) through (*c*) The forming heights are equal to (a) 1 cm, (b) 2 cm, and (c) 3 cm.

(2) The postforming RRA temper produced the highest yield strength and the smallest elongation for the same extent of superplastic deformation, which showed the peak-

Table IV. Mechanical and Stress-Corrosion Properties of Superplastically Formed Workpieces With Various Equivalent Tensile Strain

Temper*	UTS** (MPa)	0.2YS** (MPa)	El.** (Pct)	$El._{Air}$† (Pct)	$0.2YS_{Sol.}$‡ (MPa)	$El._{Sol.}$** (Pct)	$El._{Sol.}$ loss§ (Pct)
1-AC	**413.4**	**199.8**	**10.1**	—	—	—	—
2-AC	**406.8**	**192.4**	**9.5**	—	—	—	—
3-AC	**349.2**	**139.8**	**8.8**	—	—	—	—
0-T6	559.4	502.4	13.8	15.1	480.5	6.6	56.3
1-T6	551.7	490.7	11.5	12.8	474.7	5.2	59.4
2-T6	545.9	482.0	9.7	10.8	469.8	4.0	63.0
3-T6	538.9	473.6	8.6	9.3	272.3	2.4	74.2
0-RRA	**562.4**	**516.7**	**10.5**	**11.3**	**509.1**	**10.4**	**8.0**
1-RRA	**557.6**	**511.2**	**9.2**	**10.1**	**506.4**	**9.1**	**9.9**
2-RRA	**549.3**	**505.1**	**7.9**	**8.5**	**496.1**	**7.3**	**14.1**
3-RRA	**540.8**	**497.2**	**6.8**	**7.3**	**481.5**	**5.6**	**23.3**
0-T73	510.4	455.5	10.9	12.0	450.3	11.2	6.6
1-T73	506.7	453.6	9.8	10.8	448.9	10.0	7.4
2-T73	500.9	450.3	8.0	8.8	445.1	7.9	10.2
3-T73	491.1	443.8	7.4	8.0	431.2	6.7	16.3

*0, 1, 2, and 3 represent the forming height of the pan-shaped workpieces (units: cm); AC represents superplastic forming, then air cooling; and T6, RRA, and T73 represent AC specimens, then postforming T6, RRA, and T73 temper, respectively.

**Tensile test at a strain rate of $\dot{\varepsilon} = 10^{-3}$/s in air.

†Tensile test at a strain rate of $\dot{\varepsilon} = 4 \times 10^{-6}$/s in air.

‡Tensile test at a strain rate of $\dot{\varepsilon} = 4 \times 10^{-6}$/s in 3.5 pct NaCl solution.

§$El._{Sol.}$ loss = 1 − ($El._{Sol.}$**/$El._{Air}$†).

aged properties. The postforming T6 and postforming T73 tempers indicated a near peakaged and an overaged condition, respectively. On the other hand, the mechanical properties were decreased with increasing the ETS for each postforming heat treatment. The influence of ETS on the decay of mechanical properties could be found to be decreased from postforming T6, RRA to T73 tempered condition.

(3) Under the same postforming T6 tempered treatment, comparing the mechanical properties of the pan-shaped specimen possessing the ETS of about 100 pct (3-T6) with those of the unformed condition (0-T6), the losses of the yield strength and elongation are 6 and 38 pct, respectively. This result indicates that the effect of the superplastic forming on the decay of elongation is larger than that on the decay of yield strength.

The stress-displacement curves of SSRT in 3.5 pct NaCl solution for all tempered conditions are shown in Figure 4. Generally, if the value of displacement is larger, it means that the SCC resistance of the alloy is better.[22] The elongation losses for all tempered conditions are also given in Table IV. From Figure 4 and Table IV, the following points should be noted: (1) The mechanical properties, tested in 3.5 pct NaCl solution, were decreased with increasing the amount of superplastic deformation for each postforming heat treatment. However, the effect of superplastic deformation on the decay of elongation is still larger than that on the decay of strength. On the other hand, the SCC susceptibility, comparing the elongation loss, was also increased with increasing the ETS under the same postforming tempered condition. (2) Under the same ETS condition, the SCC susceptibility was the most severe for postforming T6 temper, intermediate for postforming RRA temper, and minimal for postforming T73 temper. It indicates that the postforming RRA temper could effectively improve the SCC resistance of postforming T6 temper and did not sacrifice its mechanical strength. (3) The values of

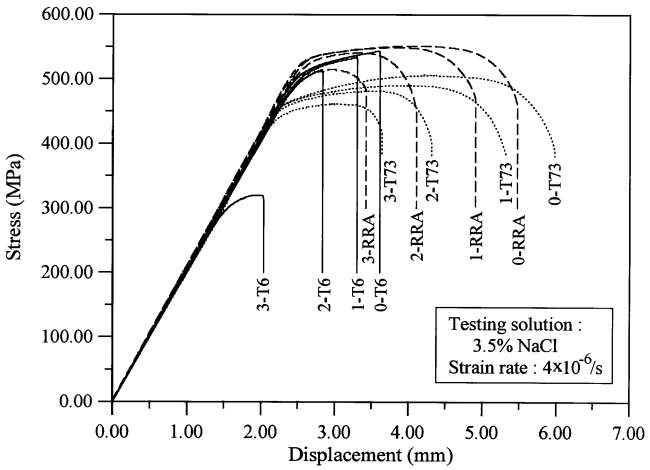

Fig. 4—Stress-displacement curves of the slow strain rate tests for various extents of superplastic deformation with different postforming heat treatments. (Each of the tempered conditions is the same as given in the footnote of Table IV.)

displacement were in proportion to the values of elongation loss for all tempered conditions. These proportional relationships proved that the relative SCC susceptibility for all tempers could be directly obtained by comparing the values of displacement of each heat treatment.

The polarization curves for different postforming heat treatments are shown in Figure 5. The electrochemical data, including corrosion potential, pitting potential, corrosion current density, and passive current density, for all tempered conditions are indicated in Table V. The following points should be noted from Figure 5 and Table V: (1) Under the same postforming heat treatment, increasing the extent of ETS caused both the corrosion potential and the pitting potential to become more anodic and both the corrosion current density and the passive current density to increase. (2) The corrosion potentials for the same amount

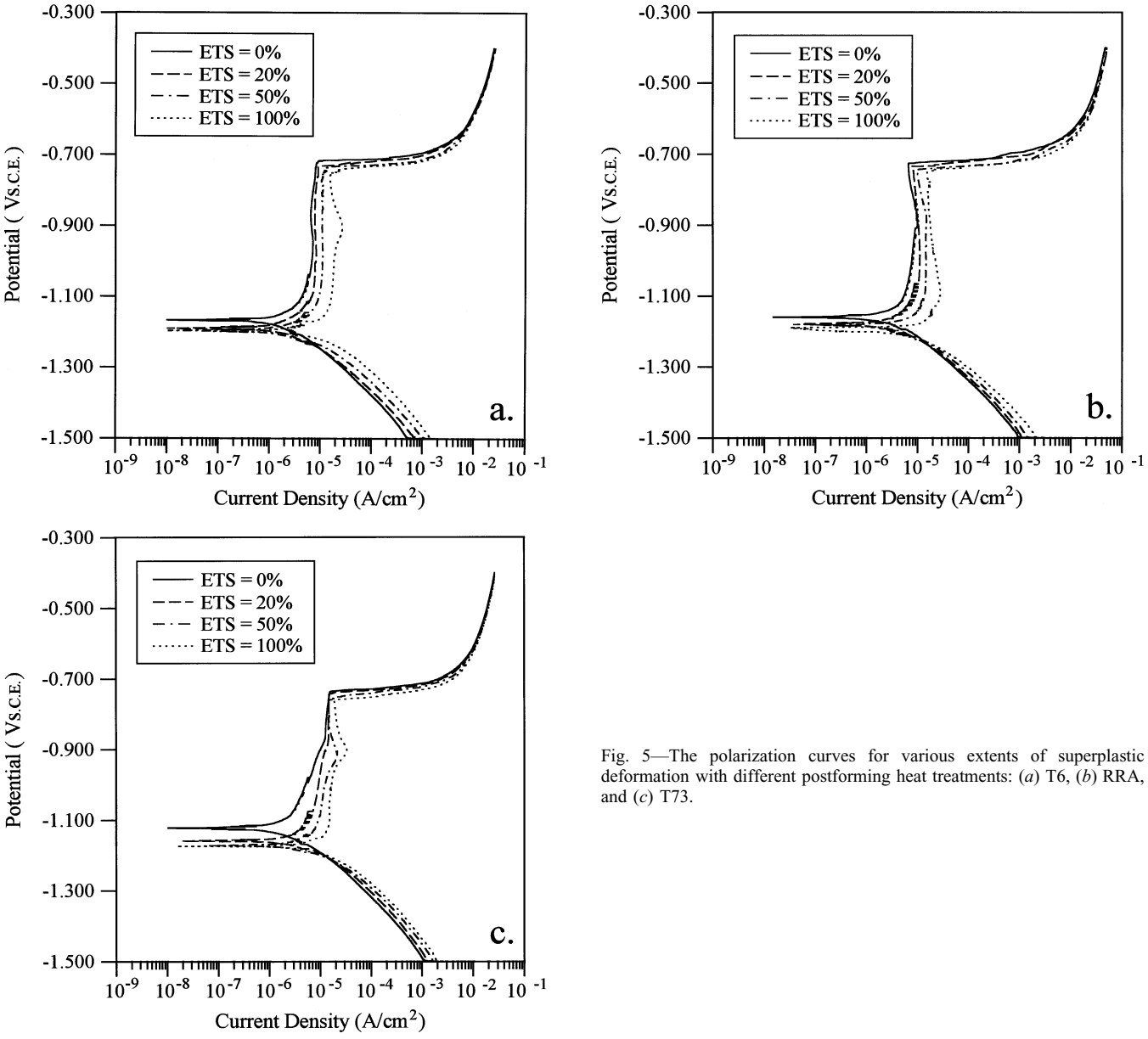

Fig. 5—The polarization curves for various extents of superplastic deformation with different postforming heat treatments: (*a*) T6, (*b*) RRA, and (*c*) T73.

of superplastic deformation were shifted to be more noble in the sequence of postforming T6, RRA, and T73 tempered condition. However, the tendency of the pitting potential for all postforming tempers in the same ETS condition is converse to that of the corrosion potential. Therefore, the range of the passive potential for the same ETS condition was decreased from postforming T6, RRA to T73 tempered. (3) Under the same ETS condition, the corrosion current density and the passive current density were decreased from postforming T6, RRA to T73 tempered. This means that the postforming T6 temper would possess the best corrosion resistance under the same extent of superplastic deformation.

After the polarization test, the typically corroded morphologies of the superplastically formed specimens are shown in Figure 6. Under the same postforming tempered condition, any obvious morphologic distinction could not be found for the different amounts of superplastic deformation. For the postforming T6 tempered specimens, the corrosion morphologies showed that the nonuniform distributions of pits with fourfold symmetry on {001} planes were formed, as indicated in Figures 6(a) and (b), respectively.[23] The corroded morphologies of the postforming RRA and T73 tempered conditions are similar to that of the postforming T6 tempered condition, as shown in Figures 6(c) through (f). However, the pitting area and the pile density of cubic pits are increased as the degree of aging is increased. It indicates that the postforming T73 temper caused the most serious pitting corrosion for the same superplastic forming condition.

The typical precipitate-free zone (PFZ) widths, grain boundary η precipitates, and slip behaviors for the pan-shaped workpieces under various postforming tempered conditions are shown in Figure 7. The PFZ width and the size of GBP were increased from postforming T6, RRA to T73 temper. However, both the slip band spacing and the slip band length revealed the opposite tendency, as did the PFZ width. No obvious microstructural difference was found for the various ETS conditions that were treated by the same postforming tempered condition.

IV. DISCUSSION

Adding the Zn and Mg alloying elements to the aluminum solid solution matrix will cause the corrosion potential of the aluminum alloy to become more anodic.[23,24] The concentration of Zn and Mg alloying elements in the matrix will be decreased with increasing the degree of aging because of the precipitation of $MgZn_2$. Therefore, the corrosion potential for the same extent of superplastic deformation would become more noble from postforming T6, RRA to T73 tempered condition, as shown in Table V. The semicoherent η' and incoherent η precipitates are well known to be more anodic than the matrix of the aluminum alloy.[24,25] It is found that by increasing the degree of aging from the postforming T6 to the postforming T73 temper, the average size and volume fraction of the more anodic η' and η precipitates were increased, but the distributed number and distributed uniformity of those precipitates were decreased. Generally, when the constituents are small, present in the greatest number, and uniformly distributed throughout the matrix, maximum corrosion resistance can be obtained.[25] Therefore, under the same ETS condition, the postforming T73 heat treatment could reveal the highest corrosion current density. Table V also shows that the pitting potential would become more negative, and the pitting current density would increase from postforming T6, RRA to T73 temper as in the same ETS condition. These results indicate that the precipitations of the η' and η can reduce the stability of passive film and promote the pitting occurrence.

The different amounts of superplastic deformation were treated by the same postforming temper, which possessed the same microstructures. This means that the formation of cavitation is the major factor causing the decay of the mechanical properties and the SCC resistance when the ETS is increased for each postforming heat treatment. It is reasonable to understand that the cavitations will become the sites of stress concentration and crack initiation to cause the decay of mechanical properties. In addition, the corrosion reaction will also occur easily around the cavitations. Increasing the extent of superplastic deformation, resulting in the higher density of the cavitation, would increase the corrosion current density for the same postforming tempered condition. The cavitation can also break the continuity of the surface Al_2O_3 film and reduce the stability of the passive film. It caused both the corrosion potential and the pitting potential to shift to more anodic, and the passive current density to be increased with increasing the ETS under the same postforming tempered condition.

The SCC susceptibility of the 7475Al alloy is mainly controlled by the hydrogen-induced cracking mechanism.[9] The RRA treatment can effectively improve the SCC resistance of T6 temper for superplastic 7475Al alloy because RRA temper can produce larger sizes of both the matrix precipitates and GBPs than can T6 tempered condition.[7] The larger diameter of GBPs in the RRA treatment can effectively trap the atomic hydrogen in bubbles nucleated at GBPs, and the larger size of the matrix precipitates will cause a decrease in the length and density of dislocation lines. These results can reduce the hydrogen concentration at grain boundary to below a critical value to inhibit hydrogen embrittlement and improve SCC resistance.[11,12,16]

Table V. Electrochemical Data of the Superplastically Formed Workpieces with Various Equivalent Tensile Strain

Temper*	ϕ_{corr}** (V)	ϕ_p** (V)	$\Delta\phi$** (V)	i_{corr}** (μA/cm^2)	i_p** (μA/cm^2)
0-T6	−1.166	−0.718	0.448	3.16	6.50
1-T6	−1.189	−0.730	0.459	4.47	7.87
2-T6	−1.196	−0.742	0.454	10.01	10.82
3-T6	−1.198	−0.758	0.440	17.78	19.31
0-RRA	**−1.158**	**−0.726**	**0.432**	**4.89**	**7.86**
1-RRA	**−1.180**	**−0.734**	**0.446**	**11.03**	**9.88**
2-RRA	**−1.182**	**−0.745**	**0.437**	**15.92**	**13.26**
3-RRA	**−1.189**	**−0.758**	**0.431**	**27.38**	**19.82**
0-T73	−1.121	−0.735	0.386	5.61	8.51
1-T73	−1.158	−0.741	0.417	13.96	10.46
2-T73	−1.171	−0.752	0.419	20.85	14.13
3-T73	−1.173	−0.760	0.413	28.51	20.17

*See Table IV.

**ϕ_{corr}: corrosion potential; ϕ_p: pitting potential; $\Delta\phi$: the range of the passive potential = $\phi_p - \phi_{corr}$; i_{corr}: corrosion current density; and i_p: passive current density.

Generally, the cathodic reaction of Al-alloy corrosion is the reduction of hydrogen ions. The atomic hydrogen produced from the corrosion reaction could become the main source of inducing the hydrogen embrittlement. The SCC susceptibility would be increased when the stress corrosion testing environment became more corrosive, as previously reported by some researchers.[26,27,28] Therefore, in the same microstructure, a more serious corrosion reaction due to superplastic forming means that more atomic hydrogen would be generated, then transported and stored up at the intersection of dislocation and grain boundary by mobile dislocations.[9] It indicates that increasing the extent of superplastic deformation will increase the SCC susceptibility under the same postforming tempered condition. In other words, the elongation loss, as indicated by a comparison of the elongation tested in air with that tested in solution, was increased with increasing the extent of ETS, as shown in Table IV. Therefore, the benefit of improving the SCC resistance of the superplastically formed workpiece by means of postforming RRA or T73 temper would be decreased with increasing the amount of superplastic deformation.

The following conclusions about the influence of superplastic deformation on the SCC can be deduced from the previous discussions: The superplastically formed workpiece should be treated by a suitable postforming heat treatment, such as RRA tempered treatment, to improve the mechanical strength and reduce SCC susceptibility. However, the cavitations followed by the superplastic forming influence not only the mechanical properties but also the corrosion and SCC resistances. Increasing the extent of superplastic deformation, which creates more cavitations, can result in the severe decay of the corrosion properties and of the SCC resistance. The advantage of improving the SCC resistance while not sacrificing the strength by means of the postforming RRA tempered condition will be decreased with increasing the extent of superplastic deformation. Therefore, it is important to pay attention to the effect of cavities on the SCC susceptibility. Improving and using a suitable superplastic forming technique, such as hydrostatic pressure, to reduce the formation of cavitation is necessary. Bampton *et al.*[3,20] showed that the cavitation

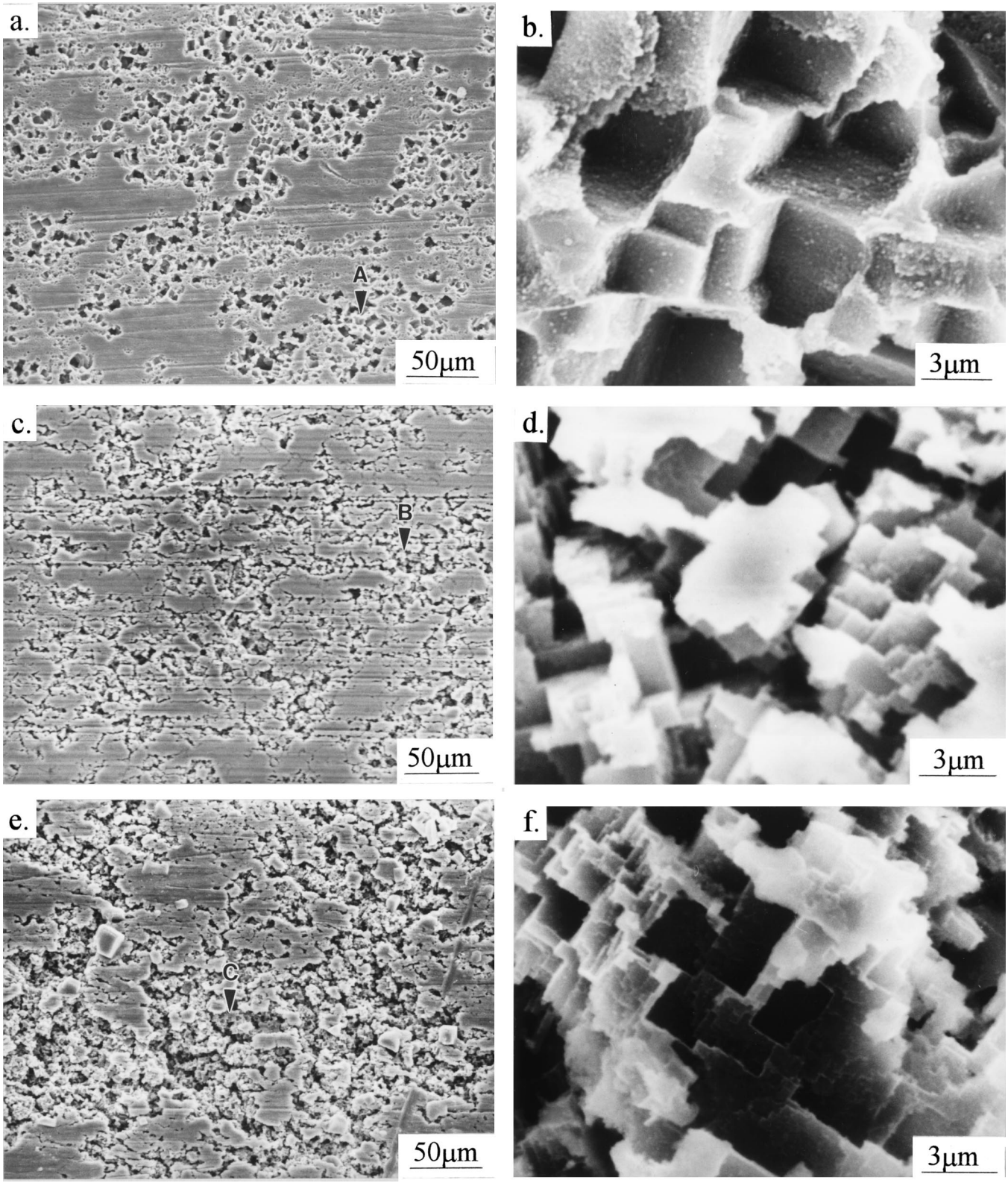

Fig. 6—The typical corrosion morphologies of the superplastically formed specimens with various postforming heat treatments: (*a*) T6, (*b*) higher magnification of area A in (a), (*c*) RRA, (*d*) higher magnification of area B in (c), (*e*) T73, and (*f*) higher magnification of area C in (e).

could be suppressed by using a back pressure. Reducing the formation of cavitation could retard the serious SCC damage when the superplastically formed workpiece is applied in a corrosive environment.

V. CONCLUSIONS

1. Under the same post-tempered condition, the mechanical properties are decreased with increasing the extent of

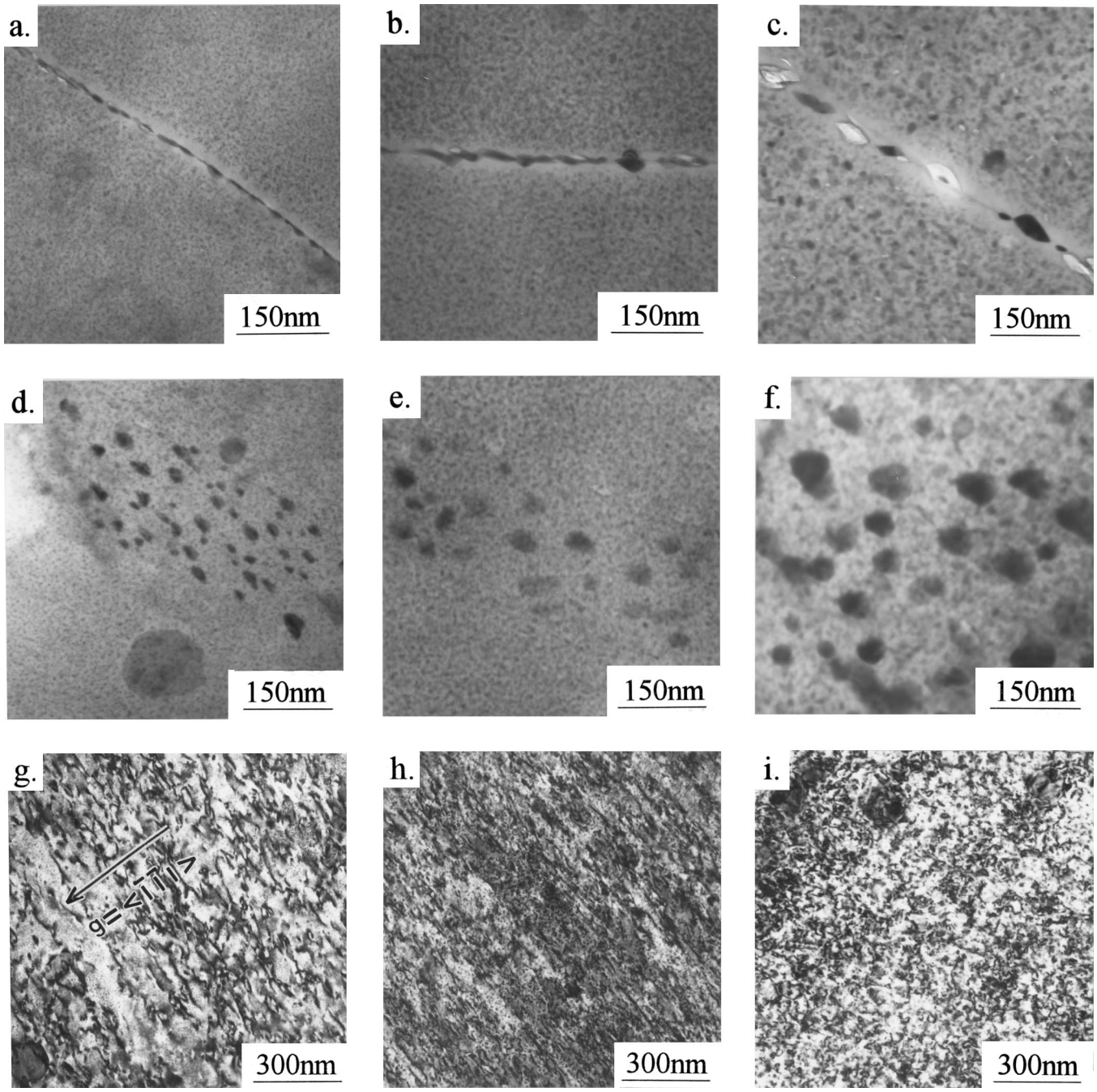

Fig. 7—(*a*) through (*c*) TEM micrographs showing the PFZ width of the various postforming tempers: (*a*) T6, (*b*) RRA, (*c*) T73, (*d*) through (*f*) showing the grain boundary precipitates of the various postforming tempers (d) T6, (e) RRA, and (f) T73; and (*g*) through (*i*) showing the deformation structure after 4 pct plastic strain for the various postforming tempers (g) T6, (h) RRA, and (i) T73. [112] matrix zone axis and g = $\langle 1\,\bar{1}\,1 \rangle$ for all micrographs.

superplastic deformation. The influence of cavitation on the decay of elongation of the superplastically formed workpieces is greater than that on the decay of its strength.

2. The SCC susceptibility is the most severe for postforming T6 temper, intermediate for postforming RRA temper, and minimal for postforming T73 temper under the same extent of superplastic deformation. The postforming RRA temper can effectively improve the SCC resistance of postforming T6 temper and does not sacrifice mechanical strength. However, the SCC resistance is decreased with increasing the extent of superplastic deformation for each postforming temper. The benefit of improving the SCC resistance by means of the postforming RRA tempered condition will be decreased if the extent of superplastic deformation is increased.
3. Increasing the amount of superplastic deformation, resulting in higher density of cavitation, would cause both the corrosion potential and the pitting potential to become more anodic, and the increase of both the corrosion current density and the passive current density for the same postforming tempered condition. A more vigorous corrosion reaction of the materials due to super-

plastic deformation is the main factor to increase the SCC susceptibility.

4. The SSRT results indicated that it is necessary to pay attention to the SCC susceptibility of the superplastically formed workpieces. These workpieces need not only a suitable post heat treatment, such as RRA tempered treatment, but also an appropriate superplastic forming technique to reduce the formation of cavitation and retard serious SCC susceptibility.

ACKNOWLEDGMENTS

The authors are grateful for the support of the National Science Council of the Republic of China under Contract Nos. NSC 82-0405-E002-099 and NSC 83-0416-E002-020.

REFERENCES

1. J.A. Wert, N.E. Paton, C.H. Hamilton, and M.W. Mahoney: *Metall. Trans. A*, 1981, vol. 12A, pp. 1267-76.
2. *Superplasticity and Superplastic Forming*, C.H. Hamilton and N.E. Paton, eds., TMS, Warrendale, PA, 1989.
3. C.C. Bampton and R. Raj: *Acta Metall.*, 1982, vol. 30, pp. 2043-53.
4. M.W. Mahoney, C.H. Hamilton, and A.K. Ghosh: *Metall. Trans. A*, 1983, vol. 14A, pp. 1593-98.
5. C.C. Bampton and J.W. Edington: *J. Eng. Mater. Technol.*, 1983, vol. 105, pp. 55-60.
6. W. Gruhl: *Z. Metallkd.*, 1984, vol. 75, pp. 819-26.
7. T.C. Tsai and T.H. Chuang: *Metall. Mater. Trans. A*, 1996, vol. 27A, pp. 2617-27.
8. T.D. Burleigh: *Corrosion*, 1991, vol. 47, pp. 89-98.
9. D. Nguyen, A.W. Thompson, and I.M. Bernstein: *Acta Metall.*, 1987, vol. 35, pp. 2417-25.
10. J. Albrecht, I.M. Bernstein, and A.W. Thompson: *Metall. Trans. A*, 1982, vol. 13A, pp. 811-20.
11. J.K. Park and A.J. Ardell: *Metall. Trans. A*, 1984, vol. 15A, pp. 1531-43.
12. L. Christodoulou and H.M. Flower: *Acta Metall.*, 1980, vol. 28, pp. 481-87.
13. G.M. Scamans, R. Alani, and P.R. Swann: *Corr. Sci.*, 1976, vol. 16, pp. 443-59.
14. B.M. Cina: U.S. Patent 3856584, Dec. 24, 1974.
15. M.U. Islam and W. Wallace: *Met. Technol.*, 1983, vol. 10, pp. 386-92.
16. K. Rajan, W. Wallace, and J.C. Beddoes: *J. Mater. Sci.*, 1982, vol. 17, pp. 2817-24.
17. M.T. Cope, D.R. Evetts, and N. Ridley: *Mater. Sci. Technol.*, 1987, vol. 3 pp. 455-61.
18. L.B. Duffy, J.B. Hawkyard, and N. Ridley: *Mater. Sci. Technol.*, 1988, vol. 4, pp. 707-12.
19. R.N. Parkins, F. Mazza, J.J. Royuela, and J.C. Scully: *Br. Corros. J.*, 1972, vol. 7, pp. 154-67.
20. C.C. Bampton, M.W. Mahoney, C.H. Hamilton, A.K. Ghosh, and R. Raj: *Metall. Trans. A*, 1983, vol. 14A, pp. 1583-91.
21. N.A. Pratten: *J. Mater. Sci.*, 1981, vol. 16, pp. 1737-1747.
22. S. Ohsaki and T. Takahashi: *J. Jpn. Inst. Light Met.*, 1985, vol. 35, pp. 261-68.
23. M. Yasuda, F. Weinberg, and D. Tromans: *J. Electrochem. Soc.*, 1990, vol. 137, pp. 3708-15.
24. S. Maitra and G.C. English: *Metall. Trans. A*, 1981, vol. 12A, pp. 535-41.
25. H.P. Godard: *Mater. Perf.*, 1981, July, pp. 9-15.
26. P.N. Adler, R. Deiasi, and G. Geschwind: *Metall. Trans.*, 1972, vol. 3, pp. 3191-3200.
27. R. Hermann: *Corrosion*, 1988, vol. 44, pp. 685-90.
28. W.T. Tsai, J.B. Duh, J.J. Yeh, J.T. Lee, and Y.C. Chang: *Corrosion*, 1990, vol. 46, pp. 444-9.